

## PRELIMINARY STUDIES ON THE SELECTIVE ABSORPTION OF CO<sub>2</sub> FROM CH<sub>4</sub> THROUGH HOLLOW FIBER MEMBRANE CONTACTOR USING AQUEOUS EXTRACT OF NONI FRUIT (MORINDA CITRIFOLIA)

Sutrasno Kartohardjono<sup>1\*</sup>, Yuliusman<sup>1</sup>, Desiana Setia Budhie<sup>1</sup>

<sup>1</sup> *Department of Chemical Engineering, Faculty of Engineering, Universitas Indonesia, Kampus Baru UI Depok, 16424*

(Received: December 2010 / Revised: January 2011 / Accepted: June 2011)

### ABSTRACT

The study has been conducted to evaluate the effectiveness of the natural solvent from noni fruit for CO<sub>2</sub> gas absorption from CH<sub>4</sub> through hollow fiber membrane gas-liquid contactors. The solvent was made of 100 grams noni fruit per liter of water. In experiments, the solvent flowed to the shell side of the contactor, while the gas mixture flowed to the lumen fiber. The experimental results showed that mass transfer coefficients in the contactors increased with increasing liquid flow rate and decreasing number of fibers in the contactors. Mass transfer correlation indicated that the mass transfer in the contactor was dominated by turbulent flow. Hydrodynamics analysis of the contactors showed that at the same Reynolds number pressure drops increased with increasing packing density due to an increase in friction between fibers and water. The friction factor ratio data revealed that the fiber surface did not behave like a smooth pipe within the range of velocities in the experiments. Based on QI and Cussler coefficients, chemical absorption occurred during experiments, which might be indicated by the appearance of new compounds in the chemical analysis of the aqueous extract from noni fruit after absorption.

*Keywords:* Hollow fiber membrane contactor; Hydrodynamic; Mass transfer; Noni

### 1. INTRODUCTION

Currently, fossil fuels supply about 80% of the world's total energy resources and produce approximately 60% of the world's electricity. However, the burning of fossil fuels produces air pollutant emissions and releases CO<sub>2</sub>, a greenhouse gas that has been associated with global climate change. From an environmental perspective it is important to capture CO<sub>2</sub> to prevent global warming threat, which is in compliance with emission reduction targets established in the Kyoto Agreement. In addition, the concentration of CO<sub>2</sub> has a wide range in natural gas. While the concentration of CO<sub>2</sub> produced from gas power plants is typically about 3-5%, it is approximately 13-15% when using coal. The need for CO<sub>2</sub> by the commercial sector, such as trade markets and enhanced oil recovery (EOR) techniques, also make the process capture of CO<sub>2</sub> important (Wang et al., 2004a).

There are many current carbon dioxide capture technologies based on physical and chemical processes such as absorption, adsorption, cryogenic and membrane technologies. The conventional CO<sub>2</sub> removal method is by absorption into an amines solution using an absorption column such as packed tower, spray tower, and bubble column (Wang et al., 2004b). The conventional column has several weaknesses, including large energy consumption and

---

\* Corresponding author's email: sutrasno@eng.ui.ac.id, Tel. +6221-7863516, Fax. +6221-7863515

problems in operations like flooding, loading, channeling, foaming, and entrainment (Al-Marzouqi et al., 2008). Membrane technology is promising and potential in the CO<sub>2</sub> separation and recovery process. This technology is more economical because it has lower capital and operational costs. The membrane used as the gas-liquid contactor is the hollow fiber membrane, which is a synthetic fiber made of polypropylene polymer. This membrane is hydrophobic so water cannot wet the membrane during the contact process. The driving force for the mass transfer in the hollow fiber membrane contactor is the difference in concentration between phases in the contactor. The contact process between the liquid and gas phase is non-dispersive, meaning there is no direct contact between the solvent and CO<sub>2</sub> so that solvent regeneration can take place easily. To prevent direct contact between two fluids, solvent flows in one side of the membrane and the other fluid containing components to be removed flows in the other side of membrane.

The most popular method for CO<sub>2</sub> removal from natural gas is via an absorption process using amine solution in a contacting device. Weak base amines are compounds that react with CO<sub>2</sub> to form weak chemical bonds, and this chemical bonding can easily be broken by warming, which is foundational for regenerating the amine compounds. Although chemical absorption technology plays an important role in the commercial aspect, the competitive selection of an absorbent which can absorb large amounts of CO<sub>2</sub> and which has a high mass transfer and low cost of regeneration is still a major challenge in the process of absorption of CO<sub>2</sub> (Xiao et al., 2000). The aims of this study are to analyze the potential of noni fruit (*Morinda citrifolia*) as the absorbent for CO<sub>2</sub> and to evaluate the effectiveness of the CO<sub>2</sub> absorption process through the hollow fiber membrane contactor based on mass transfer and hydrodynamics studies.

## 2. MATERIAL AND METHODS

The solvent used in this experiment was simply made by mixing 100 grams of noni fruit juice in 1 liter of water. CO<sub>2</sub> used in the experiment was a gas mixture of CO<sub>2</sub> and CH<sub>4</sub> (31% and 69%, respectively) from BOC gas. The membrane used was a polypropylene fiber of 2 mm in outside diameter and 0.1 μm in porosity. Sample analyses of the solvent from noni fruit were conducted before and after CO<sub>2</sub> absorption using Gas Chromatography-Mass Spectroscopy (GC/MS). Three contactors of 1.6 cm in diameter were used in the experiment, each contained 5, 12 and 16 fibers, with a fiber length of 40 cm. Figure 1 shows schematically the experimental setup used for the absorption experiments. The CO<sub>2</sub> and CH<sub>4</sub> gas mixture was sent to the lumen fiber in the contactor via a Sierra Top Trak mass flow meter and the flow was maintained at 180 SCCM (standard cubic centimeters per minute). Meanwhile, the solvent was pumped to the shell side of the contactor with a flow rate range of 350-600 Liters per hour (LPH).

Mass transfer coefficient from the experiment was calculated using Equation (1),

$$K_L = \frac{Q_L}{A} \ln \frac{C^* - C_0}{C^* - C_1} \quad (1)$$

where  $Q_L$  and  $A$  are solvent flowrate and membrane surface area, respectively. Meanwhile  $C^*$ ,  $C_0$  and  $C_1$  are CO<sub>2</sub> concentrations in solvent at equilibrium, reservoir and solvent leaving the contactor. Mass transfer correlation in the membrane contactor is usually expressed in terms of Sherwood and Reynolds numbers,

$$Sh = f(\varphi)Re^n \quad (2)$$

where  $Sh$ ,  $Re$  and  $\varphi$  are Sherwood number, Reynolds number and membrane packing fraction in the contactors, respectively. More over,  $Sh$ ,  $Re$  and  $\varphi$  are calculated using the equations below:

$$Sh = k_L \frac{de}{D} \quad (3)$$

$$\text{Re} = \frac{\rho v_L de}{\mu} \quad (4)$$

$$\varphi = n_f \frac{d_f^2}{d_p^2} \quad (5)$$

A hydrodynamic study was also conducted to observe energy loss characteristics in the hollow fiber membrane contactors. The liquid pressure drop in the contactor is expressed in the equation,

$$\Delta P = \frac{2fl\rho v_L^2}{de} \quad (6)$$

where  $\Delta P$  and  $f$  are pressure drop and friction factor,  $l$  and  $\rho$  are contactor length and liquid density, while  $v_L$  and  $de$  are liquid velocity and equivalent contactor diameter.

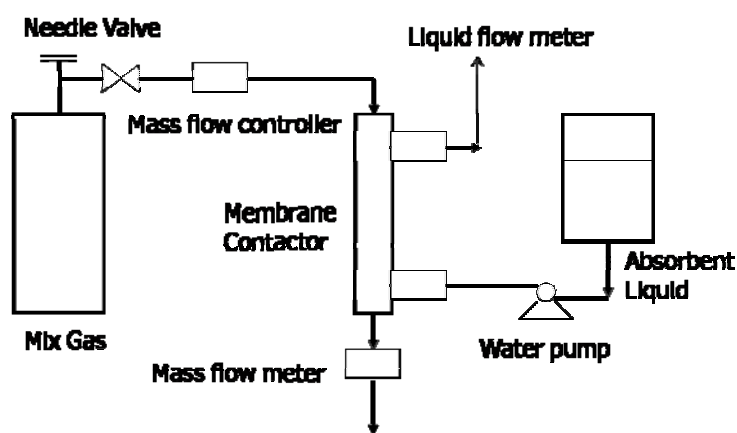


Figure 1 Schematic diagram of experimental set up

### 3. RESULTS AND DISCUSSIONS

The effect of solvent flow rates on mass transfer coefficients is shown in Figure 2 and it can be seen that mass transfer coefficients increased with increasing solvent flow rates in the membrane contactors. In the case of gas absorption in hollow fiber membrane contactors, the controlling resistance for mass transfer was usually concentrated in the liquid phase. By increasing the liquid velocity, mass transfer resistances were reduced and an increase in the overall mass transfer coefficient was observed (Dindore et al., 2004).

Figure 2 also shows that mass transfer coefficients decreased when the number of fibers in the contactors decreased. In a region of low packing density contactors transverse flow and surface renewal effect seemed to be more influential to the mass transfer performance rather than than channelling effect, while at the higher packing density the channelling effect was more dominant (Lipnizki & Field, 1999). It is possible that the geometrical dependencies of boundary layer profiles might also increase the mass transfer coefficient of a module with lower packing density. The increase would be directly related to the boundary layer conditions, where the profiles of boundary layers on a curved body become thinner with an increasing degree of curvature, such as decreasing do fiber with other conditions constant. Based on this theory, the mass transfer coefficient will increase with decreasing packing density of the module, especially at higher liquid velocities. In this study the channelling occurred because of the existing regions of dense and loose packing in the module, which created preferential flow

around fibers due to an uneven distribution of fibers and flow (Wu & Chen, 2000). Membrane contact area might have been reduced in densely packed regions as fibers were more adhered to each other, reducing the available contacting surface.

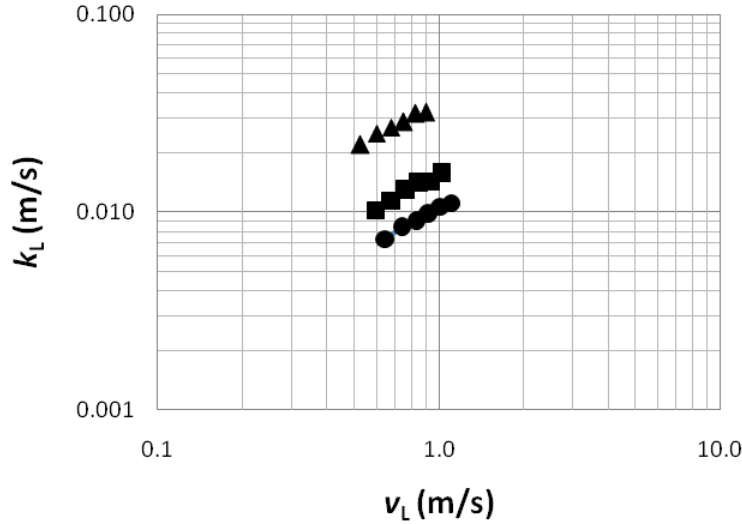


Figure 2 Variation of overall mass transfer coefficients,  $k_L$ , for the contactors consist of 5 (▲), 12 (■) and 16 fibers (●), and liquid flowrates,  $v_L$

To examine the dependence of mass transfer coefficients on the process parameters, correlations are conveniently expressed in terms of the dimensionless Sherwood number,  $Sh$ , the Reynolds number,  $Re$ , and the Schmidt number,  $Sc$ . The general equation to correlate these parameters is expressed by Equation (7),

$$Sh = A Re^B Sc^C \quad (7)$$

In this study the Schmidt number,  $Sc$ , was not varied, so the  $1/3$  power-dependence in the literature was assumed (Gabelman & Hwang, 1999), and Equation (7) become,

$$Sh = A Re^B Sc^{0.33} \quad (8)$$

Equation (8) can be more simplified to Equation (9),

$$Sh = a Re^b \quad (9)$$

where  $a$  is equal to  $f(\varphi)$ , as stated in Equation (2).

Figure 3 shows the experimental data as  $Sh$  plotted against  $Re$  at various packing densities to obtain the exponent for the Reynolds number,  $b$  in Equation (9) for each contactor. The exponent  $b$  was obtained by the linear regression illustrated in Figure 3; values ranged from 0.70 to 0.79, and the average value was 0.75.

These values were then plotted against the packing density of the module in Figure 4 and had an average value of  $b=0.75$ , indicating that mass transfer in the contactor was dominated by turbulent flow. The values of  $a$  for each contactor were obtained from the slope of the experimental Sherwood number against  $Re^{0.75}$  as shown in Figure 4; values ranged from 0.08 to 0.25. The correlation between  $a$  and the packing fraction of the contactor was obtained in the same way and is best fitted by Equation (10).

$$f(\varphi) = 0.11 \varphi^{-1.16} \quad (10)$$

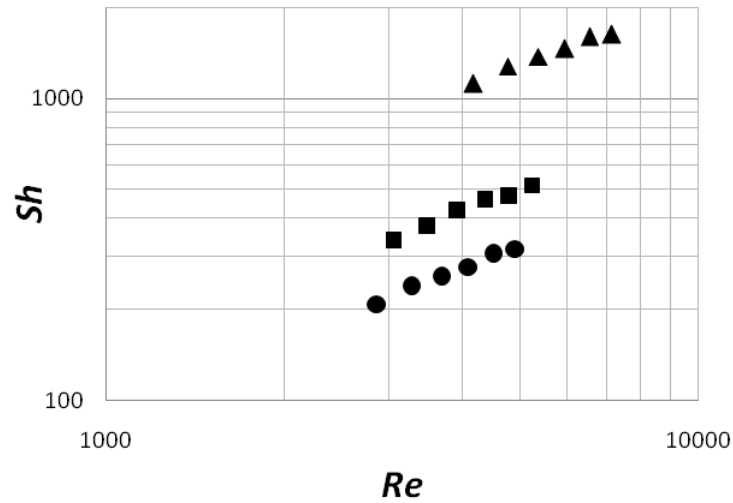


Figure 3 Variation of Sherwood number,  $Sh$ , for the contactors consist of 5 (▲), 12 (■) and 16 fibers (●), and Reynolds number,  $Re$

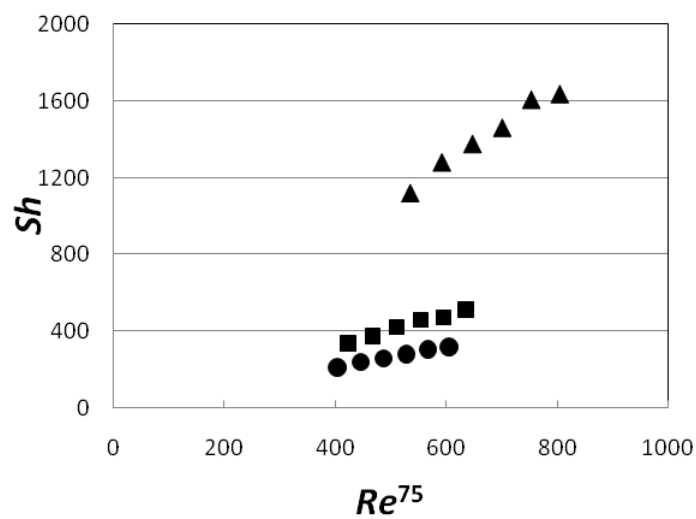


Figure 4 Variation of Sherwood number,  $Sh$ , for the contactors consist of 5 (▲), 12 (■) and 16 fibers (●), and Reynolds number,  $Re^{0.75}$

Equation (11) describes the geometric dependency of the hollow fiber membrane contactors employed in this study where mass transfer performance was related to the packing fraction of fibers in the contactors. An empirical correlation for mass transfer performance in hollow fiber membrane contactors can then be correlated in the form,

$$Sh = 0.11 \phi^{-1.16} Re^{0.75} \tag{11}$$

The energy lost for fluids flowing in the hollow fiber membrane gas liquid contactors was dominated by energy lost in the liquid phase. For the liquid flow through the lumen fibers the pressure drop was due to the friction between the liquid and the fibers. Meanwhile, for the shell side flow there were some other factors influencing the pressure drop, such as friction between water and module housing, loss due to entrance and exit of water from the module, and loss due to expansion and contraction (Ahmed et al., 2000).

In the experiments, water pressure drops in the membrane contactors were measured by a digital manometer. The pressure drop was plotted against the Reynolds number in Figure 5 to observe the effect of flow to the contactor pressure drop. Figure 5 illustrates that, at the same Reynolds number, pressure drops increased with increasing contactor-packing density due to an increase in friction between fibers and water. The increase in packing density will reduce the equivalent diameter  $d_e$ , and available area for water flow which will increase water velocity at the same Reynolds number. Based on Equation (6) pressure drop increases with decreasing equivalent diameter of the contactor and increasing water velocity.

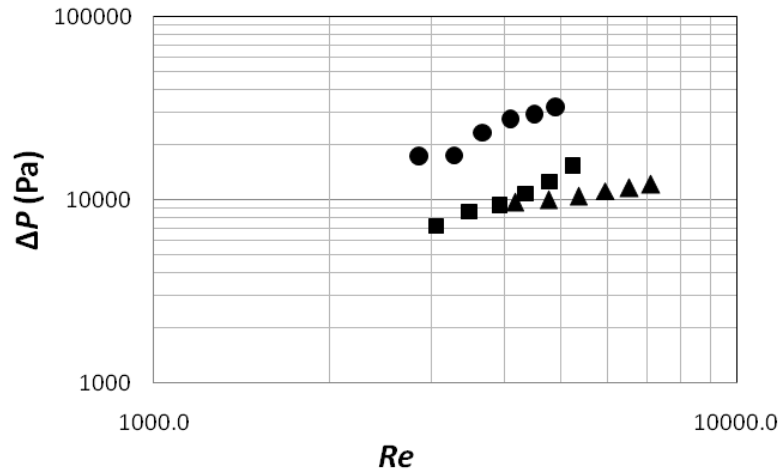


Figure 5 Variation of pressure drop,  $\Delta P$ , for the contactors consist of 5 (▲), 12 (■) and 16 fibers (●), and Reynolds number,  $Re$

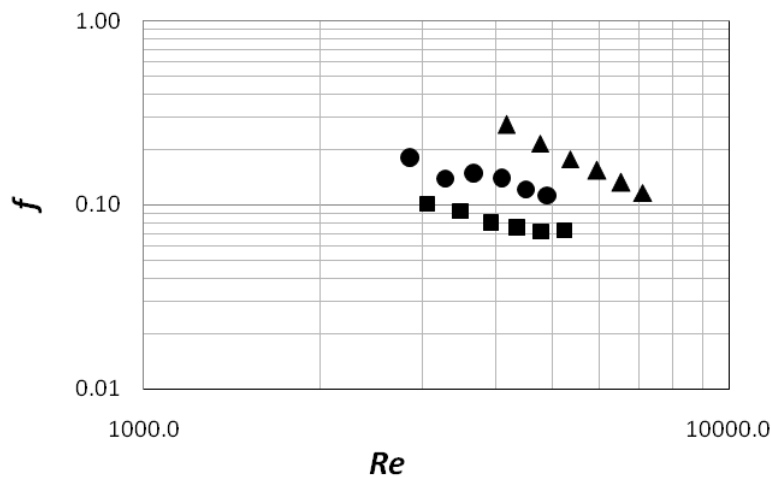


Figure 6 Variation of friction factor,  $f$ , for the contactors consist of 5 (▲), 12 (■) and 16 fibers (●), and Reynolds number,  $Re$

To evaluate the effects of contactor packing density on pressure drop due to friction loss, the friction factors of the module were obtained from Equation (6) and then were plotted against Reynolds number as shown in Figure 6. The friction factor increased with decreasing module-packing density for the same module diameter due to an increase in hydraulics diameter of the module as expressed in Equation (6).

The friction factor ratio of the module to the smooth pipe is shown in Figure 7. These data reveal that the fibers surface did not behave like a smooth pipe within the range of velocity in the experiments. The viscous sub layer did not develop due to the movement of the fibers as quantitatively expressed in very low viscous drag values compared to inertial drag values. Furthermore, the friction factor ratio decreased because the Reynolds number's dependency on the friction factor in both systems was different. The friction factors obtained for the membrane contactors in this study were 7.6 to 27.6 times higher than the theoretical value based on flow of fluids in the smooth pipe as shown in Figure 7.

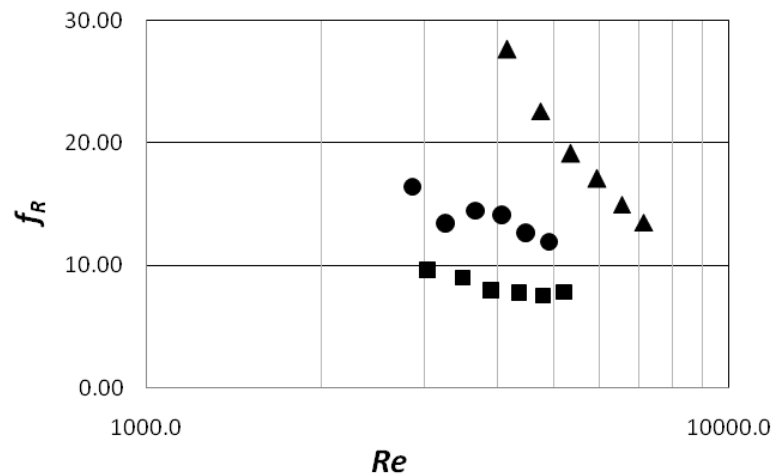


Figure 7 Variation of friction factor ratio,  $f_R$ , for the contactors consisting of 5 (▲), 12 (■) and 16 fibers (●), and Reynolds number,  $Re$

As comparison, Wickramasinghe et al. (2002) reported that the friction factor of hollow fiber blood oxygenators was about 7 times higher than the theoretical value at  $Re < 5$  and about 31 times higher than the theoretical value at  $5 < Re < 100$ . Meanwhile, Ahmed et al. (2000) reported that the friction factor of sealed end polypropylene hollow fiber modules with packing densities of 8.7 to 9.6% were about 2 times higher than the values for pipe flow reported in the literature. It can be seen here that the friction factor ratio can vary from contactor to contactor depend on the geometry of the contactors.

To examine the degree of separation that could be achieved by the hollow fiber membrane contactors used in the experiments, outlet gas analysis was carried out for the contactor consisting of 16 fibers and a liquid flow rate of 600 LPH. This condition was chosen because it gives the highest mass transfer coefficient. Based on GC analysis it was found that  $CO_2$  concentration in the gas stream can be reduced from 31% at the feed side to 10% at the contactor gas outlet.

To determine the effectiveness of the solvent used, the type of absorption that occurred during the absorption process was tested. For physical absorption, transfer of  $CO_2$  gas took place mainly by diffusion from the gas bulk, across the fiber and then to the liquid bulk. For chemical absorption, chemical reactions occurred between  $CO_2$  gas and chemical substances in the solvent. The QI and Cussler coefficient  $\left(\frac{4k_L}{d_f v_L}\right)$  was used to predict the type of absorption during the process (Qi & Cussler, 1985). A QI and Cussler coefficient  $> 1$  indicated the process was chemical absorption, and vice versa. Experimental results showed that the value of QI and

Cussler coefficients were in the range of 9.5 and 39.3, indicating that chemical absorption occurred during the CO<sub>2</sub> absorption process in the aqueous extract of noni fruits.

Chemical analyses of the aqueous extract of noni fruits using GCMS were also conducted before and after absorption, as shown in Tables 1 and 2. Chemical analyses of the solvent before and after absorption process have yet to prove that the type of absorption is chemical, as indicated by Qi and Cussler coefficients. However, some new compounds appeared in the after-absorption analysis such as 2-Furancarboxaldehyde, 5-(hydroxymethyl) and 2-Methyl-1-thiacyclohept-2-ene 1-oxide Thiepin; the appearance might indicate reactive results between CO<sub>2</sub> gas and chemical compounds in the aqueous extract of noni fruits.

Table 1 Chemical composition of aqueous extract of noni fruit before absorbing CO<sub>2</sub>

Peak	Retention Time	% Area	Library / ID	Match Quality (%)
3	4.71	2.41	4H-Pyran-4-one, 2,3-dihydro-3,5-dihydroxy-6-methyl	80
4	4.91	54.05	Octanoid acid	90
9	6.58	1.57	Decanoid acid	94
17	10.87	0.75	Hexadecanoic acid	83
19	11.11	8.83	Hexadecanoic acid (CAS) \$\$ Palmitic acid	99
20	11.36	2.96	2H-Benzopyran-2-one, 7-hydroxy-6-methoxy	96
21	12.25	1.50	9-Octadecenoic acid, (E)-\$\$ trans-delta (sup 9)	92
23	12.36	3.05	Octadecanoic acid (CAS) \$\$ Stearic acid	90

Table 2 Chemical composition of aqueous extract of noni fruit after absorbing CO<sub>2</sub>

Peak	Retention Time	% Area	Library / ID	Match Quality (%)
5	5.00	53.65	Octanoid acid	95
7	5.46	2.91	2-Furancarboxaldehyde, 5-(hydroxymethyl)	72
10	6.45	0.71	2-Methyl-1-thiacyclohept-2-ene 1-oxide \$\$ Thiepin	83
11	6.59	1.81	Decanoid acid	96
27	11.11	5.46	n-Hexadecanoic acid	98
29	11.36	3.96	2H-Benzopyran-2-one, 7-hydroxy-6-methoxy	96
30	12.25	3.47	Octadec-9-enoic acid	92
31	12.37	1.90	Octadecanoic acid	99

#### 4. CONCLUSIONS

This study was conducted to evaluate the performance of hollow fiber membrane contactors to remove carbon dioxide from a gas mixture using an aqueous extract of noni fruit (*Morinda citrifolia*) and water. Experimental results showed that mass transfer coefficients in the contactors increased with increasing liquid flow rates and decreasing numbers of fibers in the contactors. Mass transfer correlation indicated that the mass transfer in the contactor was dominated by turbulent flow. A hydrodynamics analysis of the contactors showed that, at the same Reynolds number, pressure drops increased with increasing packing density due to an increase in friction between fibers and water. The friction factor ratio data reveals that the

surface of the fibers did not behave like a smooth pipe within the range of velocities in the experiments. Based on QI and Cussler coefficients, chemical absorption occurred during the experiments, which might be indicated by the appearance of new compounds in the chemical analysis of the aqueous extract of noni fruit after absorption.

## 5. REFERENCES

- Ahmed, T., Semmens, M.J., Voss, M.A., 2000. Energy Loss Characteristics of Parallel Flow Bubbleless Hollow Fiber Membrane Aerators. *Journal of Membrane Science*, 171(1): pp. 87-96.
- Dindore, V.Y., Brillman, D.W.F., Feron, P.H.M., Versteeg, G.F., 2004. CO<sub>2</sub> Absorption at Elevated Pressures using a Hollow Fiber Membrane Contactor. *Journal of Membrane Science*, 235(1-2): pp. 99-109.
- Gabelman, A., S.-T. Hwang, 1999. Hollow Fiber Membrane Contactors. *Journal of Membrane Science*, 159(1-2): pp. 61-106.
- Lipnizki, F., Field, R.W., 1999. Simulation and Process Design of Pervaporation Plate-and-Frame Modules to Recover Organic Compounds from Waste Water. *Chemical Engineering Research and Design*, 77(3): pp. 231-240.
- M. H. Al-Marzouqi, M.H.E.-N., S.A.M. Marzouk, M.A. Al-Zarooni, N. Abdullatif, R. Faiz Al-Marzouqi, 2008. Modelling of CO<sub>2</sub> Absorption in Membrane Contactors. *Separation and Purification Technology*, 59: pp. 286-293.
- Qi, Z., Cussler, E.L., 1985. Microporous Hollow Fibers for Gas Absorption : I. Mass Transfer in the Liquid. *Journal of Membrane Science*, 23(3): pp. 321-332.
- Wang, R., Li, D. F., Liang, D. T., 2004a. Modeling of CO<sub>2</sub> Capture by Three Typical Amine Solutions in Hollow Fiber Membrane Contactors. *Chemical Engineering and Processing*, 43(7): pp. 849-856.
- Wang, R., Li, D. F., Zhou, C., Liu, M., Liang, D. T., 2004b. Impact of DEA Solutions with and without CO<sub>2</sub> Loading on Porous Polypropylene Membranes Intended for Use as Contactors. *Journal of Membrane Science*, 229(1-2): pp. 147-157.
- Wickramasinghe, S.R., B. Han, 2002. Mass and Momentum Transfer in Commercial Blood Oxygenators. *Desalination*, 148(1-3): pp. 227-233.
- Wu, J., Chen, V., 2000. Shell-side Mass Transfer Performance of Randomly Packed Hollow Fiber Modules. *Journal of Membrane Science*, 172(1-2): pp. 59-74.
- Xiao, J., Li, C.-W., Li, M.-H., 2000. Kinetics of Absorption of Carbon Dioxide into Aqueous Solutions of 2-amino-2-methyl-1-propanol+monoethanolamine. *Chemical Engineering Science*, 55(1): p. 161-175.